

### TECHNICAL UNIVERSITY OF CIVIL ENGINEERING OF BUCHAREST

### **FACULTY OF RAILWAYS, ROADS AND BRIDGES**

# DYNAMIC RESPONSE OF A FOOTBRIDGE TO THE WIND DYNAMIC ACTION

**IONESCU P. GABRIELA** 

## DYNAMIC RESPONSE OF A FOOTBRIDGE TO THE WIND DYNAMIC ACTION

#### Abstract:

Footbridges are mainly subjected to the action of the wind and pedestrians in their everyday life. The recent developments in material technology and efficient construction techniques enable the construction of not only longer but also lighter and more slender footbridges. Therefore, the modern suspended footbridges have become more prone to vibrations due to the wind actions. Several researchers have introduced models to explain the phenomenon of synchronous lateral excitation of footbridges, but there is no consensus on the general applicability of these models. Hence, there is still effort to model the pedestrian-footbridge behaviour in order to understand this complex phenomenon.

**Keywords:** wind, footbridge, vibration, frequency.

#### 1.Introduction

Classy, luminossity and slenderness are words which, in general, characterise the modern architecture. Neither the footbridges are an exception to this trend. Their increasing span and the materials characteristics they are made of, increasengly lighter, give them extra particularity. Bridges, whether they are road, rail or pedestrian, fixed or mobile, always exert an attraction on human imagination. Indeed, there are structures that through conception, execution technology and aesthetics have been landmarks in the evolution of constructions. From the monumentality of a Roman aqueduct (Fig. 1) to the elegance of a modern

footbridge (Fig. 2), we note the evolution over centuries of these constructions that highlight the progress in knowledge and the evolution of the materials used.





Fig.1. Pont du Gard aqueduct, France

Fig.2. Footbrigde, Israel

A suspended bridge for outstanding pedestrians, to be noted here, is the Millenium Bridge over the Thames River in London, because it has a special composition versus the classic solution we are used to (Fig.3). The recently constructed artwork has a length of 320.00 m and a span of 144.00 m which is not a performance, but it is noted that the pillars do not far exceed the level of the path and the path is not sustained by the tie by the carrier cable supports on transverse frames supported on carrier cables.



Fig.3. Millenium Pedestrian Bridge over the River Thames, England

The study of vertical and lateral oscillations of footbridge pedestals generated by pedestrian action and wind action is a topic of great interest in the scientific and technical community over the past ten years. An important number of papers were published on the one hand on experimental studies on footbridge already carried out and on the interpretation of the results of tests performed on experimental platforms. In this regard, this article attempts to synthesize some aspects of the problem of the dynamic action of wind on suspended pedestrian bridges.

The suspended footbridge is a modern structure with high flexibility. In order to evaluate the response of this structure to the dynamic wind action it was necessary to conduct a linear geometric analysis in a dynamic regime.

#### 2. Description of the analyzed structure

The suspended bridge under consideration is a footbridge with bicycle tracks, with three spans (50.00 + 150.00 + 50.00) m, with a total length of 250.00 m and a useful width of 3.00 m (Fig.4).

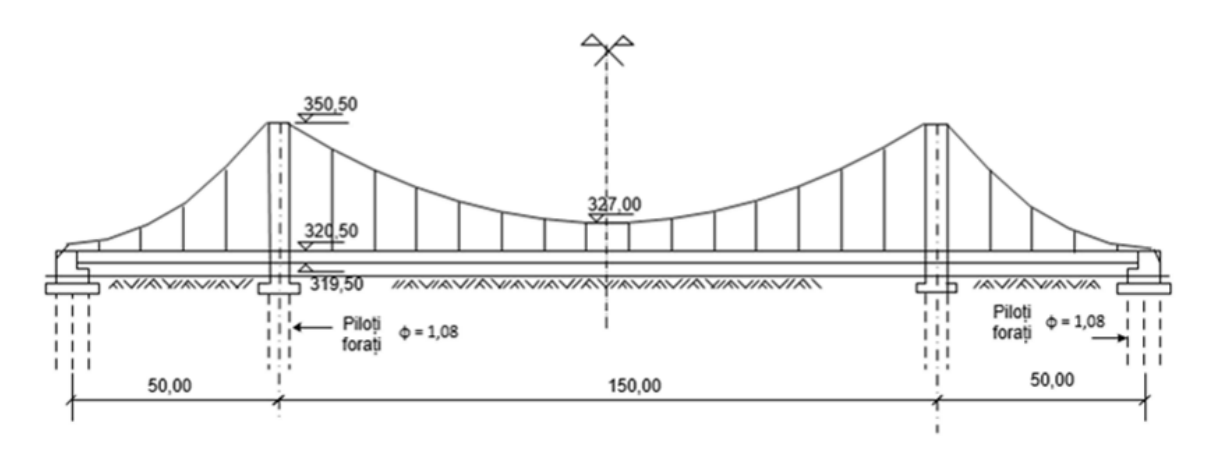
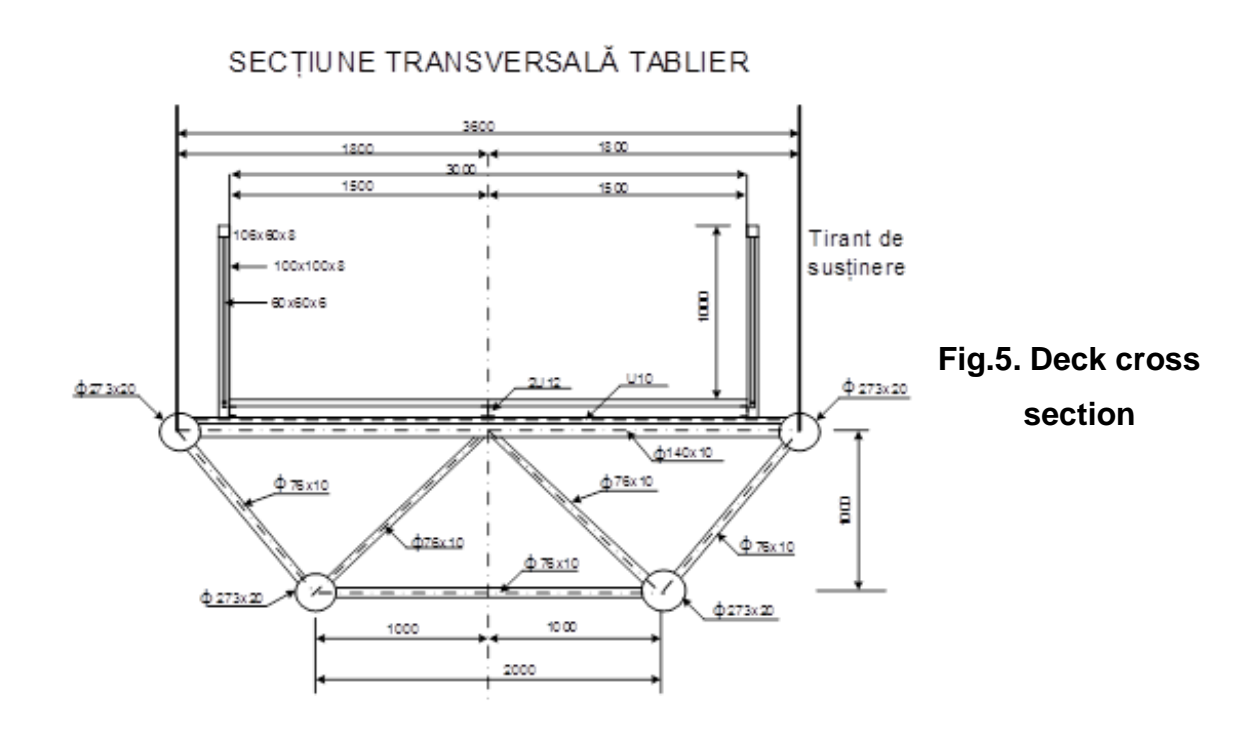
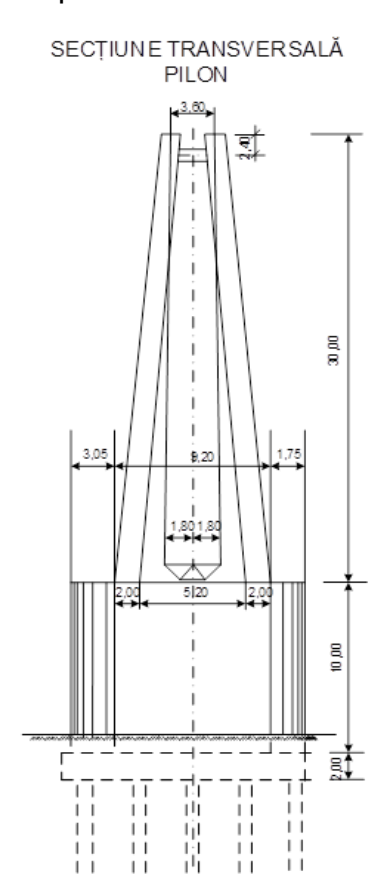


Fig.4.Static general layout of the pedestrian bridge

The deck has a height of 1.00 m and is made in a girder with metal circular pipe girder with a 10 mm thick steel deck (fig.5).



The footbridge suspension system consists of the main cables having a parabolic shape and each of 6 carrier cables with a diameter of  $\varphi$  = 44mm and the support



struts made of round steel with a diameter of  $\phi$  = 40mm with lengths varying between 605 mm and 21830 mm measured between the gripping points. Pylons are made of reinforced concrete with rectangular cross-section of 2.00 m x 3.50 m, and 30.00 m above the table (Fig.6).

Fig.6. Pillar cross section

#### 3. Description of the discreet calculation model approached

Structure modeling and dynamic analysis of the analyzed system were made using the London University Stress Analysis System (LUSAS) developed by the British company Finite Element Analysis Ltd [1].

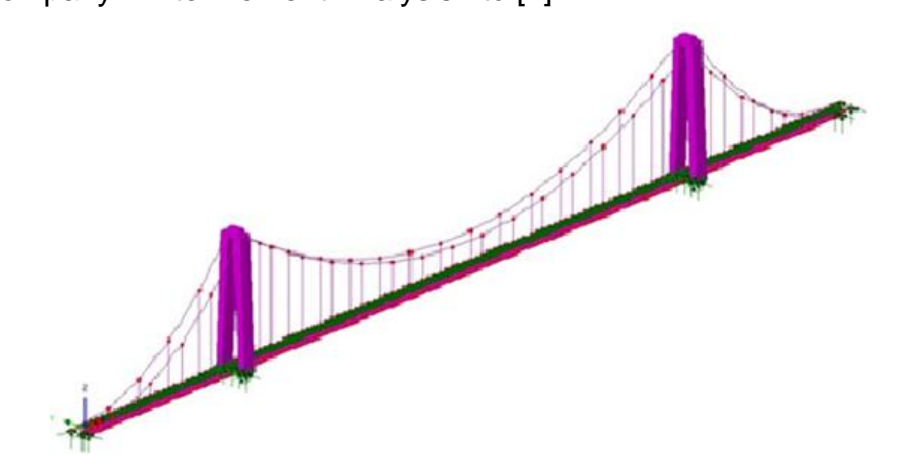


Fig.7. Configuration of the discreet calculation model at the suspended footbridge

For the analyzed structure, the bridge map for pedestrians was modeled using two-dimensional "Thick Shell" quad-square quadrilater (QTS4) for the steel

deck, and one-dimensional "Thick Beam" (BMS3) finishing elements for all lattice bars (main longitudinal beams, beams transversal, diagonal and bracing). Pylons and reinforcing beams were modeled with 3D "thick beam" finite elements. The discrete model (Fig. 7) thus composed contains 3116 finite elements, 4278 knots, resulting in 8108 degrees of dynamic freedom.

#### 3.1. Materials used

1. S235 steel having 210 GPa elastic modulus, density 7850 kg / m3 and Poisson 0.3 coefficient for metallic elements; 2. Steel with 180 elastic modulus, density 7850 kg / m3 and Poisson 0.3 coefficient for cables; 3. C45 / 55 reinforced concrete with 36 GPa elastic modulus, density 2548.4 kg / m3 and poisson 0.2 poles. All materials have linear behavior.

#### 4. Analysis of eigenvalues and eigenvectors. Own vibration characteristics

An analysis of its eigenvalues and eigenvectors has been carried out, the results of which are presented below, starting with tabulated frequencies for the main vibration modes and ending with modal modalities for the analyzed structure.

Densitatea	Modul propriu de vibrație	Valori ale frecvențelor funcție de modul de aplicare al pietonilor și densitatea aglomerării [Hz]			
aglomerării (pietoni/m²)		Fără pietoni	Pietoni pe toate deschiderile	Pietoni numai pe deschiderea centrală	
0.5		Modul 1 0.742247	0.705372	0.705547	
8.0	Modul 1		0.685707	0.685965	
1.0			0.673470	0.673775	
0.5			0.946768	0.946933	
8.0	Modul 2	0.996608	0.920235	0.920476	
1.0			0.903738	0.904023	
0.5	Modul 3	Modul 3 1.49338	1.41866	1.41970	
8.0			1.37889	1.38040	
1.0			1.35416	1.35594	
0.5			1.93089	1.93414	
0.8	Modul 4	14 2.02887	1.87825	1.88297	
1.0			1.84536	1.85093	
0.5			1.95460	1.95953	
8.0	Modul 5	Modul 5 2.05741	1.89986	1.90704	
1.0			1.86582	1.87429	

Table 1. Frequency values of their vibration modes resulting from the modal analysis of the suspended footbridge

Frequency calculation (Table 1) was done by modal analysis in order to determine its own vibration modes having frequencies lower than 5Hz (Table 2). For the suspended superstructure the vibration modes consisting of individual vibrations of the structure cables were not taken into account.

Table 2.Own vibration modes of the suspended footbridge

Own vibration modes	Modal Form	Frequency of the vibration mode (Hz)	Factors of mass participation	
Mode 1		0.742247	PFX	0.737874E-07
			PFY	0.396433
	Side bending of the deck on the central span		PFZ	0.806166E-11
Mode 2	Vertical bending of the deck	0.996608	PFX	0.810431E-03
			PFY	0.322511E-07
			PFZ	0.436306E-08
Mode 3	Vertical bending of the deck	1.49338	PFX	0.242769E-04
			PFY	0.568331E-09
			PFZ	0.175758

			1	
Mode 4	Torsional side bending of the deck	2.02887	PFX	0.838101E-07
			PFY	0.239134E-02
			PFZ	0.216786E-04
Mode 5	General vertical bending of the deck	2.05741	PFX	0.352752E-02
			PFY	0.294016E-06
			PFZ	0.140295
Mode 6	General vertical bending of the deck	3.06806	PFX	0.785178E-02
			PFY	0.100218E-05
			PFZ	0.214574E-04
Mode 7	Torsional side bending of the deck	3.65760	PFX	0.638141E-05
			PFY	0.218365E-01
			PFZ	0.145745E-06

			<del>-</del>
Torsion of the deck on the central span	3.82670	PFX	0.273831E-06
		PFY	0.302840E-03
		PFZ	0.225261E-08
General vertical bending of the deck	4.14665	PFX	0.828520E-02
		PFY	0.799434E-05
		PFZ	0.101068E-02
General vertical bending of the deck	4.25668	PFX	0.247809E-01
		PFY	0.559198E-09
		PFZ	0.809447E-01
Torsional side bending of the deck	4.31133	PFX	0.133108E-06
		PFY	0.958246E-03
		PFZ	0.552088E-04
	General vertical bending of the deck	Torsion of the deck on the central span  4.14665  General vertical bending of the deck  4.25668  General vertical bending of the deck  4.31133	3.82670 PFY  PFZ  Torsion of the deck on the central span  PFX  4.14665 PFY  PFZ  General vertical bending of the deck  PFX  4.25668 PFY  PFZ  General vertical bending of the deck  PFX  PFX  PFX  PFX  PFZ  PFZ  PFZ  PFZ

Mode 12	Torsional side bending of the deck	4.68205	PFX	0.253878E-05
			PFY	0.391668
			PFZ	0.162799E-05
Mode 13	General lateral bending of the deck	4.83422	PFX	0.397927E-02
			PFY	0.115007E-05
			PFZ	0.412886
Mode 14	Torsion of the deck on the central span	4.89340	PFX	0.217200E-05
			PFY	0.127977E-02
			PFZ	0.308320E-05

#### 5. Assessment loads due to wind action

For the analyzed superstructure, SR EN 1991-1-4: 2006, [2] was used for the assessment of loads due to wind action on structural elements of the suspended bridge for a wind speed of 30 m / s above a category ground II, as follows: Tablier - the force due to the wind action in the x direction was evaluated with the simplified method using the formula:  $\mathbf{F}_w = \frac{1}{2} \cdot \mathbf{\rho} \cdot \mathbf{v}_b^2 \cdot \mathbf{C} \cdot \mathbf{A}_{ref}$ . The value of the coefficient C resulted for this calculation:  $C = c_e \cdot c_{f, \, x} = 1.70 \cdot 1.30 = 2.21 \text{ and } \mathbf{A}_{ref} = 0.546 \text{ m}^2.$  Under these conditions, the resulting wind pressure on the board is  $F_w = 1.166 \text{ N}$ ; Pylon - Similarly to the board, the force due to the wind action in the x-direction was evaluated according to the same design preferences, with the simplified method

using the same calculation expression. In this case, the coefficient of wind force C is equal to the product of the coefficient of exposure, which is the force coefficient for the cylinders  $c_{f,\,0}$  and  $\Psi_{\lambda}$ , which is the factor of the end effect.  $C=C_e\cdot c_{f,\,0}\cdot \Psi_{\lambda}=2.7\cdot 1.30\cdot 0.78=2.738$ . For the given structure, the obstruction factor  $\phi$ , ie the ratio between the sum of the projections of the areas of the elements marked A and the total area of the structure labeled AC, resulted with a unitary value. Then the resultant wind pressure on the pillar is  $F_w=5.989$  N; Cables - similar to the pillars and pillars, the coefficient of wind force C has the value:  $C=c_e\cdot c_{f,\,0}\cdot \Psi_{\lambda}=2.7\cdot 0.7\cdot 0.92=1.863$  and the obstruction factor  $\phi=1$ . Then for cables  $F_w=0.0513$  N; Stringers - similar to the pillars, pillars and cables, the wind force coefficient is  $C=2.8\cdot 0.75\cdot 0.92=1.932$ . For struts  $F_w=0.0483$  N.

To simulate random stationary wind fields at any point of time and space, in a section along the bridge, NatHaz was used online [NOWS] [3] and a simulated wind history was obtained. Based on the ASCE 7-98 (American Society of Civil Engineers) on average wind speed, the NatHaz on-line simulator [NOWS] gives the user the option to download the simulation results for a dynamic analysis structural

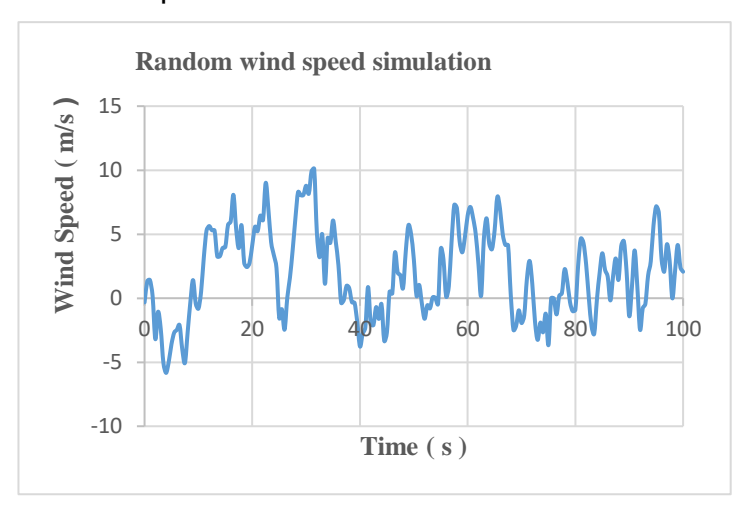


Fig.8 Random wind speed simulation

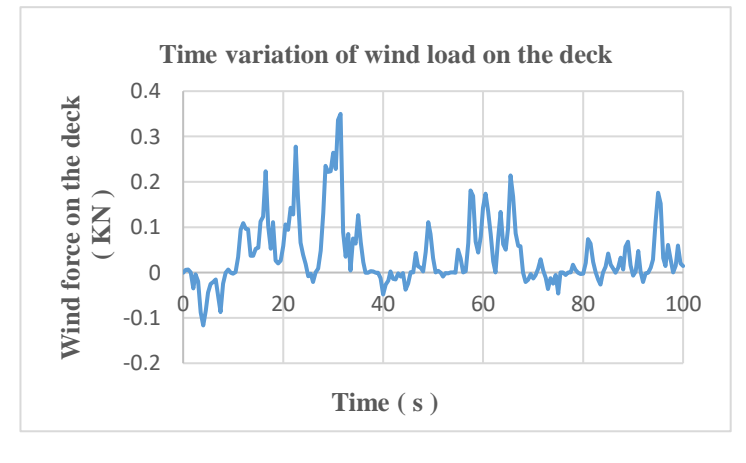
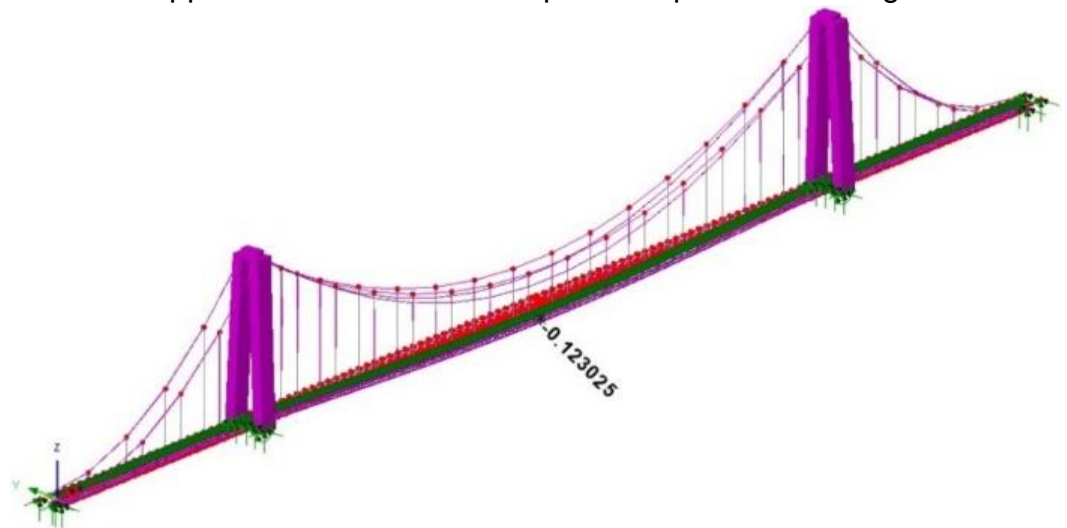


Fig.9. Time variation of wind load on the deck

under wind conditions. The wind simulator options support both metric (SI) and English units as inputs, and the location inputs for horizontal and vertical coordinates can be arbitrary but with consideration of the roughness of the terrain. The same wind simulator mentioned above was used considering that the superstructure is 10.00 m above the ground level. Figure 8 shows an example of wind speed simulation offered by NatHaz online [NOWS]. With this simulation, the wind loads according to SR EN 1991-1-1-4 were then determined with a dynamic character applied to the deformed shape of the permanent weight structure (Fig. 9).



The suspended pedestrian bridge was first loaded with its own weight resulting in a maximum vertical displacement of 12.3 cm (Fig. 10), and then on the deformed form the dynamic action of the wind resulted in the maximum positive transverse displacements (Fig. .11) and negative (Fig.12) [4].

Fig.10. Maximum vertical displacement by weight, Dz = 0.1230 m

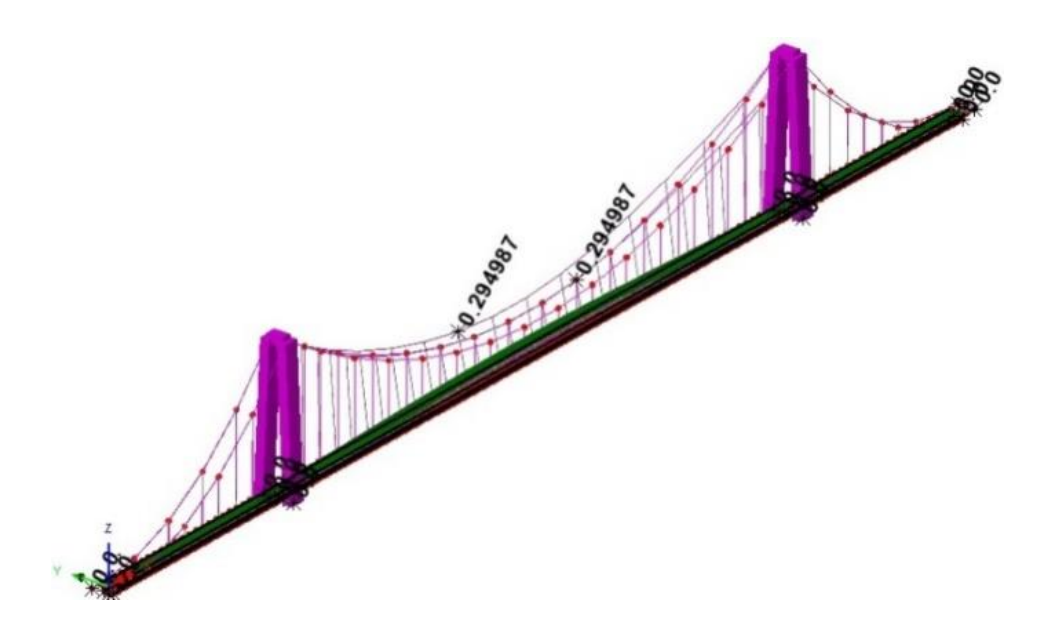


Fig.11. Positive maximum lateral displacement, Dy = 0.2949 m

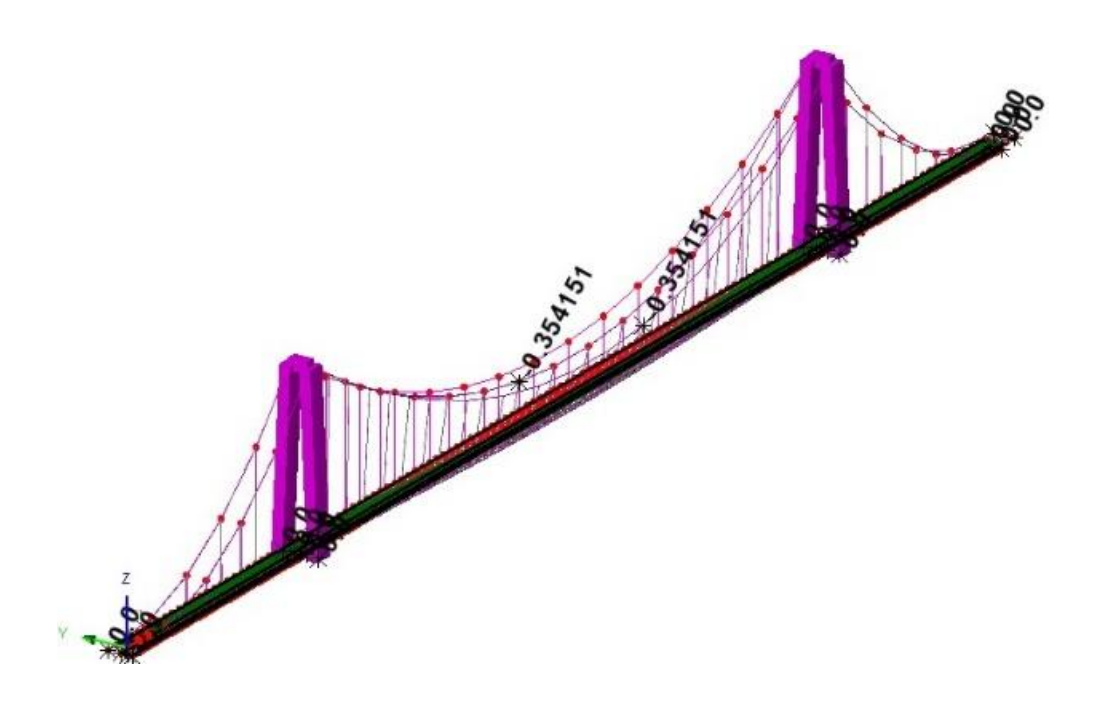


Fig.12. Negative maximum lateral displacement, Dy = 0.3541 m

#### 6. Checks on loss of aerodynamic stability

For the suspended footbridge it was determined according to [67] the critical wind velocity for the module i, for producing the phenomenon of breaking the vortices, as follows:

$$v_{crit,i} = \frac{b \cdot n_{iy}}{St} = \frac{3.60 \cdot 1.49338}{0.106} = 50.7186 \frac{m}{s}$$
,

relation in which the Strouhal St number was determined by assimilation of the cross section of the deck with a rectangular section plate having the ratio d / b = 3.60 / 0.60 = 6.

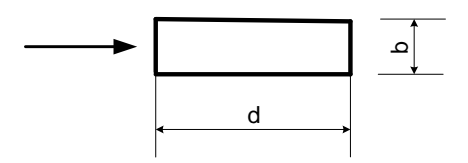


Fig.13. Illustration of the dimensions adopted for the whipping criteria

Because the ratio vcrit, i / vm = 50.7186m / s / 30m / s = 1.6906 > 1.25, the effect of vortex detachment is not examined according to [5].

The torsional divergence phenomenon is a phenomenon of instability that occurs in the case of flexible plate-like structures, such as the suspended footbridge deck, at a critical wind speed. The expression of this critical speed according to [5] is:

$$v_{div} = \sqrt{\frac{2 \cdot K_a}{\rho B^2 \left(\frac{dC_M}{d\theta}\right)}} = \sqrt{\frac{2 \cdot 49694.12}{1.25 \cdot 3.60^2 \cdot 1.36167}} = 67.123 \ m/s$$

In this last formula, in order to determine the torsional rigidity Ka was applied in the configuration of the discrete calculation model, a conventional calculation force of 100 KN at node 1083 and -100 KN at node 573 having the lever arm half the width of the board, thus a torque of 360 KNm and a rotation of the board  $\theta$  = 0.0072443 rad. Also, to determine the gradient of the aerodynamic torque coefficient relative to the rotation around the torsion center according to [5], Figure E.6 was used, respectively the formula:

$$\frac{dC_M}{d\theta} = -6.3 \left(\frac{b}{d}\right)^2 - 0.38 \frac{b}{d} + 1.6 = -6.3 \left(\frac{0.60}{3.60}\right)^2 - 0.38 \frac{0.60}{3.60} + 1.6 = 1.36167$$

We assure the condition, according to [5], that:

 $V_{div}>2~v_m(\mathbf{z}_s),$  67.123  $\frac{m}{s}>2~\cdot$  30  $\frac{m}{s}$  , so the phenomenon of divergence is not analyzed.

Next, we study the critical wind velocity corresponding to the phenomenon of flutter aerodynamic instability, according to the empirical (1.1.), (1.2.) and (1.3.), according to [6]:

The formula (1.1.): 
$$V_{co} = \left[1 + (\varepsilon - 0.5)\sqrt{\left(\frac{r}{b}\right) \times 0.72\mu}\right]\omega_b b$$

$$V_{co} = \left[1 + \left(\frac{3.82670}{1.49338} - 0.5\right) \sqrt{\left(\frac{1.453}{1.80}\right) \times 0.72 \frac{972}{3.14 \cdot 1.25 \cdot 1.80^2}}\right] 1.49338 \cdot 1.80$$

$$V_{co} = 248.9985 \, m/s$$

The formula (1.2.): 
$$V_{co} = T_{h0}^{-1} f_1 B$$
,  $cu T_{h0}^{-1} = 2.5 \left(\frac{\mu r}{b}\right)^{0.5}$  
$$V_{co} = 19.63212 \cdot 3.82670 \cdot 3.60 = 270.4544 \, m/s$$
 
$$T_{h0}^{-1} = 2.5 \left(\frac{972 \cdot 1.453}{3.14 \cdot 1.25 \cdot 1.80^2 \cdot 1.80}\right)^{0.5} = 19.63212$$

The formula (1.3.): 
$$V_{co} = 3.71 f_a B \sqrt{\left[1 - \left(\frac{f_y}{f_a}\right)^2\right] \frac{\sqrt{m I_g}}{\rho B^3}}$$

$$V_{co} = 3.71 \cdot 3.82670 \cdot 3.60 \cdot \sqrt{\left[1 - \left(\frac{1.49338}{3.82670}\right)^{2}\right] \frac{\sqrt{972 \cdot 2051.4}}{1.25 \cdot 3.60^{3}}}$$

$$V_{co} = 51.247166 \cdot 4.53045 = 232.1728 \, m/s$$

It can be seen that the three empirical relations above provide fairly appropriate values of the critical wind velocity corresponding to the waving phenomenon, even if they are very high and hence the phenomenon of loss of aero elastic stability cannot occur.

**7. Conclusions:** a). In order to increase the accuracy of the obtained results, a dynamic calculation can be approached in the non - linear domain for the analyzed structure; b) It can also be achieved by a dynamic non-linear calculation, deepening aspects related to the effects of pedestrian dynamic action on pedestrian bridge structures; c) The studies in this article represent an introduction to the analysis of pedestrian bridges for the dynamic action of the wind, having the role of exemplifying and applying current knowledge in ensuring the comfort and safety requirements for operation for these types of structures.

- [1] \*\*\* LUSAS Finite Element Analysis Ltd, User Guide, 2009
- [2] EUROCOD 1: Acțiuni asupra structurilor. Partea 1-4: Acțiuni generale Acțiuni datorate vântului, 2006
- [3] Site: <a href="http://windsim.ce.nd.edu/int\_winsim">http://windsim.ce.nd.edu/int\_winsim</a>
- [4] Cremona, C., Foucriat, J.C.- Comportement au vent des ponts, Presses de l'ecole nationale des ponts et chaussees, Paris, France, 2002;
- [5] Eurocode 1: Actions on structures Part 1-4: General actions Wind actions, 2004;
- [6] H.Wang, S.Qin, Y. Tan: Analysis of wind stability of cable-stayed bridge with single cable plane, Electrical Review, Nr 9b/2012.